2014 IEEE 17th International Conference on
Intelligent Transportation Systems (ITSC)
October 8-11, 2014. Qingdao, China

Index Modulated OFDM with Interleaved Grouping for V2X Communications

Xiang Cheng, Miaowen Wen, Liuqing Yang, and Yuke Li

Abstract— **The rapid penetration of intelligent transportation systems (ITS) into the conventional transportation infrastructure urgently calls for high spectral efficiency high reliability communication technology for vehicle-to-vehicle and vehicle-to-infrastructure (V2X) applications. Since orthogonal frequency division multiplexing (OFDM) is widely considered as a promising candidate for such applications, in this paper we propose a novel variation of OFDM for improved spectral efficiency as well as enhanced reliability in V2X channels with correlated frequency-selective fading and inevitable Doppler effects. Our proposed scheme is built upon a recently emerging technique termed as index modulated (IM-)OFDM. However, different from the existing localized subcarrier grouping, we propose interleaved subcarrier grouping. We then carry out analytical and simulated comparisons to demonstrate the merits of this new scheme in terms of both the bit error rate (BER) performance and the maximum achievable rate (MAR) of the overall system, in V2X channels.**

I. INTRODUCTION

V2X communications is envisioned to significantly empower the ITS by helping "extend a vehicle's field of vision." A vehicle that sees better on its own makes fewer demands of its driver, thus greatly enhancing safety and efficiency for everyone on the road [1], [2]. In the future, it is also expected that V2X will eventually enable vehicles to be in constant communication with its surrounding environment at various scales spanning from neighboring vehicles, traffic control centers, gas/charging stations, and even the smart cities [3]. Such rapidly growing communication needs pose stringent and urgent pressure on communication systems with improved spectral efficiency, without sacrificing communication reliability in the challenging V2X channels that are typically frequency-selective and subject to inevitable Doppler effects.

On the other hand, the most promising communications technology for V2X is widely believed to be the OFDM technique [4]–[6], which is evidenced by the worldwide adoption of the IEEE802.11p standard [7]. In this paper, we propose a novel variation of this technique to achieve higher spectral efficiency without sacrificing the system reliability.

OFDM is an appealing transmission technique, which can effectively combat the inter-symbol interference caused by the frequency-selective fading channels. The basic idea of OFDM is to divide the system bandwidth into several subbands such that each of them undergoes frequency flat fading. In the mean time, an appealing transmission technique termed as spatial modulation (SM) recently emerged for its potential of striking an attractive tradeoff between spatial spectral efficiency and energy efficiency of a wireless network [8]-[12]. Though SM was originally proposed for multi-antenna systems [13], [14], the multiple frequency channels in OFDM can be considered as the frequency-domain counterpart of the multiple spatial channels in multi-antenna systems. Hence, the concept of SM was later transplanted to OFDM systems [15]-[19].

The first attempt was made in [15], in which the so called subcarrier-index modulation (SIM-)OFDM was proposed, where the activation or de-activation of each OFDM subcarrier is used to convey one bit from the transmitter to the receiver. It is shown in [15] that SIM-OFDM can achieve up to 4 dB signal-to-noise ratio (SNR) gain over conventional OFDM for a target bit error rate (BER) under the same transmit power constraint. However, SIM-OFDM needs an error-free feed-forward link which is impractical, especially for highly-variable vehicular channels, and henceforth is prone to bit error propagation in practice [16]. To solve these problems, an enhanced SIM-OFDM scheme (ESIM-OFDM) was proposed in [16]. ESIM-OFDM allows either one of every two adjacent subcarriers to be active at a time such that one bit can be conveyed via subcarrier activation. Therefore, accounting for the N subcarriers, in total $N/2$ bits can be implicitly conveyed in determining the states of subcarriers of an OFDM signal. It is revealed in [16] that ESIM-OFDM has a lower peak-to-average power ratio (PAPR) and lower BER than conventional OFDM in an additive white Gaussian noise (AWGN) channel. However, these advantages of ESIM-OFDM come at the price of reduced spectral efficiency with respect to SIM-OFDM.

Recently, a more spectrum efficient scheme, termed as index-modulated (IM-)OFDM was proposed in [17], which can be regarded as a generalization of ESIM-OFDM. In IM-OFDM, a subset of subcarriers are activated according to the incoming information bits and the active subcarriers carry M-ary phase shift keying/quadrature amplitude modulation (PSK/QAM) symbols as in conventional OFDM. To ease the implementation of IM-OFDM, the authors suggested splitting the OFDM block into subblocks such that subcarrier activation and symbol modulation can be performed within each subblock independently. It is shown through theoretical analysis and simulations that IM-OFDM achieves signifi-

X. Cheng is with School of Electronics Engineering and Computer Science, Peking University, Beijing, 100871, China, and is also with the National Mobile Communications Research Laboratory, Southeast University, Nanjing, China (e-mail: xiangcheng@pku.edu.cn).

M. Wen is with School of Electronic and Information Engineering, South China University of Technology, Guangzhou, 510641, China (e-mail: eemwwen@scut.edu.cn).

L. Yang (Corresponding Author) and Y. Li are with the State Key Laboratory of Management and Control for Complex Systems, Institute of Automation, Chinese Academy of Sciences, Beijing, 100190, China (e-mail: liuqing.yang@ieee.org, yklee666@gmail.com).

978-1-4799-6078-1/14/$31.00 ©2014 IEEE

cantly better uncoded BER performance than conventional OFDM [19].

Note that different from OFDM, information is carried by both the active subcarrier indices and the modulated symbol riding on the active subcarriers. Hence, the selection of the grouping method can be very critical for the resulted system performance. In the existing IM-OFDM [19], each subblock is grouped by adjacent subcarriers in frequency. However, this approach does not provide any robustness against correlated frequency-selective fading, and is prone to Doppler effects which introduce interference among neighboring subcarriers. Both of these features are often present in V2X channels. Aiming at a design that is more suitable for V2X applications, in this paper we propose interleaved grouping, where well-separated subcarriers are designated into a subblock, and term it as interleaved grouping. The merit of our proposed IM-OFDM with interleaved grouping is twofold: improved spectral efficiency, and enhanced error performance in the presence of correlated frequency-selective fading and Doppler effects. Via theoretical analysis and simulated study using realistic V2X channel models, we will show that our proposed interleaved grouping facilitates a higher achievable rate than the existing localized grouping for any given modulation, and that it enhances the system reliability even in the presence of (severe) Doppler effects.

The rest of this paper is organized as follows. Section II presents the principle of IM-OFDM. Section III describes the idea of IM-OFDM with interleaved grouping. The merits of interleaved grouping over localized grouping are revealed by theoretical analysis and simulations in Section IV. Finally, concluding remarks are given in Section V.

II. SYSTEM MODEL

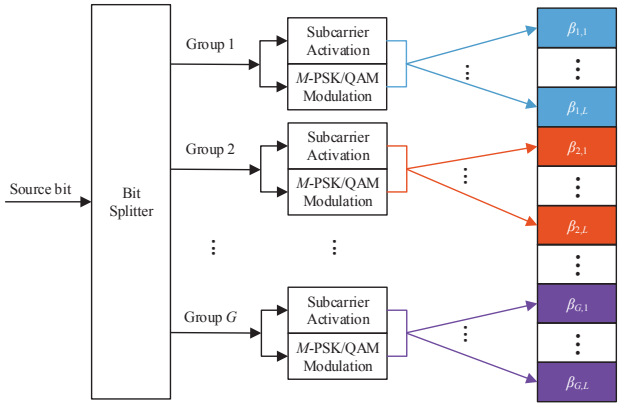

Fig. 1. Transmitter Structure of IM-OFDM with localized grouping.

Fig. 1 shows the transmitter structure of the proposed IM-OFDM in [19]. Suppose that there are a total of N OFDM subcarriers. In IM-OFDM, they are first grouped into G subblocks, each of which consisting of $L = N/G$ subcarriers. Then, subcarrier activation and symbol modulation are performed within each subblock independently. More specifically, m out of L subcarriers are set to be idle while the remaining $(L-m)$ subcarriers are activated to transmit $(L-m)$ modulated symbols drawn from M-ary PSK/QAM constellation, where M is the cardinality of the constellation. Given L and m, there are $\mathbb{C}(L,m)$ combinations of active subcarrier indices, each of which is chosen equi-probably. Hence, $\log_2 \mathbb{C}(L,m)$ bits can be conveyed via subcarrier activation. Therefore, in conjunction with the information bits carried on the $(L-m)$ modulated symbols, IM-OFDM can convey a total of $(\log_2 \mathbb{C}(L,m) + (L-m)\log_2 M)$ bits per subblock, resulting in a spectral efficiency of the system, measured in bps/Hz, as

$$f_{IM-OFDM} = \frac{\log_2 \mathbb{C}(L,m)}{L} + \frac{(L-m)\log_2 M}{L}. \quad (1)$$

Denote the subcarrier indices of the g-th $(g = 1,\ldots,G)$ subblock as $\Phi^g = \{\beta_{g,1},\ldots,\beta_{g,L}\}$. It follows that $\Phi^1 \cup \cdots \cup \Phi^G = \{1,\ldots,N\}$. Without loss of generality, assume that the j-th $(j = 1,\ldots,\mathbb{C}(L,m))$ combination of active subcarrier indices, denoted by Ω_j^g, is selected according to the incoming $\log_2 \mathbb{C}(L,m)$ information bits. Note that $\Omega_j^g \subset \Phi^g$ and $|\Omega_j^g| = L-m$. Also note that the selection can be implemented via either a look-up table or the combinatorial method proposed in [19]. Given Ω_j^g, the received signal within the g-th subblock in the frequency domain can be expressed by

$$Y_{\beta_{g,i}} = \begin{cases} H_{\beta_{g,i}} X_{g,i} + W_{\beta_{g,i}}, & \beta_{g,i} \in \Omega_j^g \\ W_{\beta_{g,i}}, & \beta_{g,i} \notin \Omega_j^g \end{cases} \quad (2)$$

where $X_{g,i}$ is the transmitted M-PSK/QAM symbol, $H_{\beta g,i}$ is the channel coefficient, and $W_{\beta_{g,i}}$ is the AWGN of variance N_0, at the $\beta_{g,i}$-th subcarrier, respectively. It is worth noting that the average transmit power of $X_{g,i}$ is $P/(L-m)$ rather than P/L as in conventional OFDM with P being the total transmit power per subblock due to the presence of inactive subcarriers.

The task of the IM-OFDM receiver is to detect the active subcarriers and the modulated symbols riding upon them. Consider the common case where the channel state information is available at the receiver. Then based on (2), the optimal ML detector can be derived as

$$\left[\hat{j}, \left\{\hat{X}_{g,i}\right\}_{\beta_{g,i}\in\bar{\Omega}_{\hat{j}}^g}\right] = \underset{X_{g,i}\in\chi, j\in\Theta}{\arg\min} \sum_{\beta_{g,i}\in\bar{\Omega}_j^g} \left|Y_{\beta_{g,i}}\right|^2 + \sum_{\beta_{g,i}\in\Omega_j^g} \left|Y_{\beta_{g,i}} - H_{\beta_{g,i}} X_{g,i}\right|^2 \quad (3)$$

where $\Theta = \{1,\ldots,\mathbb{C}(L,m)\}$, $\bar{\Omega}_j^g$ is the complement of Ω_j^g, and $\chi = \{x_1,\ldots,x_M\}$ represents the M-PSK/QAM alphabet of average power $P/(L-m)$. It is clear that the computational complexity of the ML detector in (3) is up to $\mathcal{O}\left(M^{L-m}\mathbb{C}(L,m)\right)$ per subblock since the active subcarrier indices and the modulated symbols are jointly detected. To reduce the computational complexity, a log likelihood ratio (LLR) detector is proposed in [19], whose idea is to perform the aforementioned detections in a serial manner. More specifically, the first step is to detect the state of the

$\beta_{g,i}$-th subcarrier, i.e., either active or inactive, by examining the LLR value (c.f. [19])

$$\lambda_{\beta_{g,i}} = \ln(L-m) - \ln(m) + \frac{\left|Y_{\beta_{g,i}}\right|^2}{N_0} + \ln\left(\sum_{k=1}^{M} \exp\left(-\frac{1}{N_0}\left|Y_{\beta_{g,i}} - H_{\beta_{g,i}} x_k\right|^2\right)\right). \quad (4)$$

Then, the $(L-m)$ subcarriers within the g-th subblock having maximum LLR values are determined to be active. If the collection of their indices match set $\Omega_{\widehat{j}}^{g}$, then the information index is demapped to $\widehat{j}$. The second step is to demodulate the received signals associated with the subcarriers determined to be active in the first step. It can be readily shown that the computational complexity of the LLR detector is $\mathcal{O}(LM)$ per subblock, which is the same as that of the conventional OFDM detector.

III. Principle of Interleaved Grouping

Note that different from conventional OFDM, in IM-OFDM information is carried on both the active subcarrier indices and the modulated symbols riding on the active subcarriers. Hence, the selection of the grouping method can be very critical for the resulted system performance. In [19] where the IM-OFDM scheme was originally proposed, the subcarrier grouping is performed in a localized manner, as shown in Fig. 1. In other words, neighboring subcarriers are grouped together to give $\Phi^g = \{L(g-1)+1, L(g-1)+2, \ldots, Lg\}$ with $\beta_{g,i} = L(g-1)+i$.

For communication channels in ITS that are subject to unique fading effects and inevitable Doppler, adjacent subcarriers often experience correlated fading in frequency and are subject to the most significant inter-carrier interference (ICI) caused by Doppler. Hence, the localized grouping in [19] is expected to suffer from performance degradation, especially when the coherence bandwidth spans beyond $(L-1)$ subcarriers.

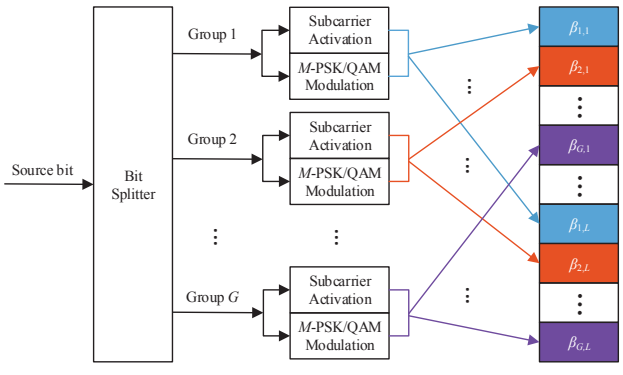

Fig. 2. Transmitter Structure of IM-OFDM with interleaved grouping.

To benefit from the frequency-selective fading, and to improve the system robustness against Doppler, we propose to group the subcarriers in an interleaved manner which results in $\Phi^g = \{g, g+G, \ldots, g+(L-1)G\}$ with $\beta_{g,i} = g+(i-1)G$, as depicted in Fig. 2. Note that when interleaved mapping is employed at the transmitter, it should also be accounted for at the receiver, as indicated in Fig. 3.

It is evident that the interleaved mapping leads to the same overall system complexity as the localized mapping. However, since the subcarriers within a group after interleaved mapping are spaced equally in a distance usually greater than the coherence bandwidth, they are likely to experience independent fading statistically. Henceforth, one should expect improved performance of the interleaved grouping when compared with the localized grouping as a frequency diversity gain can be achieved within each subblock. In the next section, we will examine and demonstrate such performance advantage in terms of both the achievable data rate and the BER, via analysis as well as simulations based on V2X channel models.

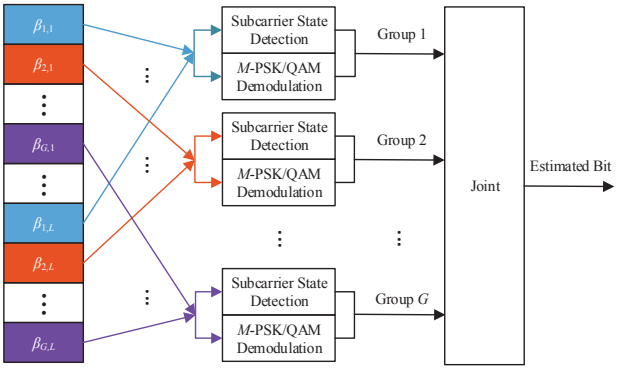

Fig. 3. Receiver Structure of IM-OFDM with interleaved grouping.

IV. Benefits of Interleaved Grouping

We will first analyze the maximum achievable data rates of IM-OFDM with localized grouping and interleaved grouping in mathematically tractable Rayleigh fading channels. Then we will resort to a simulated study to verify the envisioned BER and data rate benefits of our proposed interleaved grouping using V2X channel models.

A. The Maximum Achievable Rate

Since the encoding and decoding processes within all subblocks are independent of each other and the frequency correlation is the same for each subblock provided that either localized grouping or interleaved grouping is applied, we will only focus on one subblock in the following analysis and omit the subscript g in Ω_j^g for brevity. In addition, we let $\beta_{g,i} = i$ for notational simplicity such that all subcarriers within one subblock will be indexed from $\{1, \ldots, L\}$. Note that with the above agreement, we will refer to the i-th subcarrier simply as the $\beta_{g,i}$-th subcarrier of OFDM signals without otherwise specified.

To begin with the analysis, define $\mathbf{X}_c$ as the active subcarrier index set, $\mathbf{X}_s$ as the transmitted signal set,

$\mathbf{Y} = [Y_1, \ldots, Y_L]^T$ as the received signal set, $\mathbf{H} = [H_1, \ldots, H_L]^T$, and $\mathbf{W} = [W_1, \ldots, W_L]^T$. Assuming channel state information at the receiver and ignoring the cyclic prefix, we can derive the instantaneous mutual information (MI) of IM-OFDM as

$$\mathcal{I}(\mathbf{X}_s, \mathbf{X}_c; \mathbf{Y}|\mathbf{H}) = \mathbb{H}(\mathbf{X}_s, \mathbf{X}_c) - \mathbb{H}(\mathbf{X}_s, \mathbf{X}_c|\mathbf{Y}, \mathbf{H}) \quad (5)$$

where $\mathbb{H}(\cdot)$ denotes the entropy. Due to the independence between symbol modulation and subcarrier activation, the first term at the right hand side of (5) can be calculated as

$$\mathbb{H}(\mathbf{X}_s, \mathbf{X}_c) = (L-m)\log_2 M + \log_2 \mathbb{C}(L, m). \quad (6)$$

Towards computing the second term, let us first express it according to the definition as (7), shown at the top of the next page, where $\sum_{p^{(n)}} = \sum_{p_1}^{M} \cdots \sum_{p_n}^{M}$. Then, changing the integral variables in (7) by

$$W_i = \begin{cases} Y_i - H_i \sqrt{\frac{P}{L-m}} x_{p_{\Omega_j^{-1}(i)}}, & i \in \Omega_j \\ Y_i, & i \in \overline{\Omega}_j \end{cases}$$

we obtain

$$\mathbb{H}(\mathbf{X}_s, \mathbf{X}_c|\mathbf{Y}, \mathbf{H}) = 1 - \log_2 e + \frac{1}{L \cdot \mathbb{C}(L, m)} \frac{1}{M^{L-m}} \times \sum_{j=1}^{\mathbb{C}(L,m)} \sum_{p^{(L-m)}} \mathbb{E}_{\mathbf{W}} \left\{ \log_2 \left(\sum_{j'=1}^{\mathbb{C}(L,m)} \times \sum_{p'^{(L-m)}} \prod_{i=1}^{L} \mathcal{Q}(W_i, H_i) \right) \right\} \quad (8)$$

where $\mathbb{E}\{\cdot\}$ denotes the expectation operation and $\mathcal{Q}(W_i, H_i)$ is given by (9), shown at the top of the next page.

Having the instantaneous MAR in (5), we are now able to derive the ergodic MAR of IM-OFDM per subcarrier in average, i.e., spectral efficiency of the system, by averaging (5) over the channel as [21]

$$\overline{R}_{IM-OFDM} = \frac{L-m}{L}\log_2 M + \frac{\log_2 \mathbb{C}(L, m)}{L} - \log_2 e + 1 - \frac{1}{L \cdot \mathbb{C}(L, m)} \frac{1}{M^{L-m}} \sum_{j=1}^{\mathbb{C}(L,m)} \sum_{p^{(L-m)}} \times \mathbb{E}_{\mathbf{W},\mathbf{H}} \left\{ \log_2 \left(\sum_{j'=1}^{\mathbb{C}(L,m)} \sum_{p'^{(L-m)}} \prod_{i=1}^{L} \mathcal{Q}(W_i, H_i) \right) \right\} \quad (10)$$

where $\mathcal{Q}(W_i, H_i)$ is given by (9). Note that the spectral efficiency of conventional OFDM can be derived easily by letting $m = 0$ in (10).

From (10), we calculate the spectral efficiencies achieved by IM-OFDM with localized grouping and interleaved grouping by modeling the frequency responses as complex Gaussian random variables with zero mean and unit variance, which are highly correlated within each subblock but mutually independent across subblocks. The results are presented in Fig. 4 together with the spectral efficiency of conventional

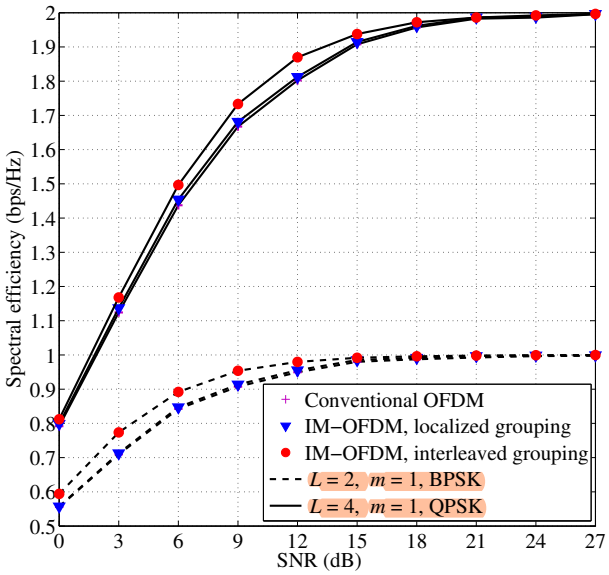

Fig. 4. Comparison between conventional OFDM and IM-OFDM with localized grouping and interleaved grouping in terms of spectral efficiency with parameters chosen as: (1) $L = 2$, $m = 1$, BPSK; (2) $L = 4$, $m = 1$, QPSK.

OFDM, where the parameters are chosen as: (1) $L = 2$, $m = 1$, with BPSK; and (2) $L = 4$, $m = 1$, with QPSK. With such parameters, IM-OFDM share the same uncoded transmitted information rate as the conventional OFDM. This explains why they all saturate at the same spectral efficiency at very high SNR. As one can observe from Fig. 4, IM-OFDM with interleaved grouping can achieve an SNR gain of up to 3 dB when compared to IM-OFDM with localized grouping. For example, such SNR gain can be observed at the spectral efficiency value of 0.95 bps/Hz for parameter set (1) and 1.9 bps/Hz for parameter set (2), respectively.

B. Performance Comparisons

Next, we carry out Monte Carlo simulations to validate the benefits of the proposed interleaved grouping method in typical V2X environments. The system parameters are listed in Table I, which are configured according to IEEE 802.11p that is one of the most promising candidates for V2X communications [7].

TABLE I
SYSTEM PARAMETERS

Parameter	Value
Signal Bandwidth	10 MHz
Carrier Frequency	5.9 GHz
Number of Total Subcarriers	64
Number of Cyclic Prefix	16
Subcarrier Spacing	156.3 kHz
OFDM Symbol Duration	8 μs

1) Channel Model: So far, V2X channels have been extensively investigated (see e.g., [22]-[30] and the references therein). In the simulations, we adopt the channel model

$$\mathbb{H}\left(\mathbf{X}_s,\mathbf{X}_c|\mathbf{Y},\mathbf{H}\right)=\frac{-M^{m-L}}{\left(\pi N_0\right)^L\mathbb{C}\left(L,m\right)}\sum_{j=1}^{\mathbb{C}(L,m)}\sum_{p^{(L-m)}}\int_{\mathbf{Y}}\prod_{i=1}^{m}e^{-\frac{\left|Y_{\Omega_j(i)}\right|^2}{N_0}}\prod_{i=1}^{L-m}e^{-\frac{\left|Y_{\Omega_j(i)}-H_{\Omega_j(i)}\sqrt{\frac{P}{L-m}}x_{p_i}\right|^2}{N_0}}$$
$$\times\log_2\left(\frac{\prod_{i=1}^{L-m}e^{-\frac{\left|Y_{\Omega_j(i)}-H_{\Omega_j(i)}\sqrt{\frac{P}{L-m}}x_{p_i}\right|^2}{N_0}}\prod_{i=1}^{m}e^{-\frac{\left|Y_{\overline{\Omega}_j(i)}\right|^2}{N_0}}}{\sum_{j'=1}^{\mathbb{C}(L,m)}\sum_{p'^{(L-m)}}\prod_{i'=1}^{L-m}e^{-\frac{\left|Y_{\Omega_{j'}(i')}-H_{\Omega_{j'}(i')}\sqrt{\frac{P}{L-m}}x_{p'_{i'}}\right|^2}{N_0}}\prod_{i'=1}^{m}e^{-\frac{\left|Y_{\overline{\Omega}_{j'}(i')}\right|^2}{N_0}}}\right)d\mathbf{Y} \tag{7}$$

$$\mathcal{Q}\left(W_i,H_i\right)=\begin{cases}2e^{-\frac{\left|W_i+H_i\sqrt{\frac{P}{L-m}}\left(x_{p_{\Omega_j^{-1}(i)}}-x_{p'_{\Omega_{j'}^{-1}(i)}}\right)\right|^2}{N_0}}, & i\in\Omega_j\cap\Omega_{j'}\\ 2e^{-\frac{\left|W_i+H_i\sqrt{\frac{P}{L-m}}x_{p_{\Omega_j^{-1}(i)}}\right|^2}{N_0}}, & i\in\Omega_j\cap\overline{\Omega}_{j'}\\ 2e^{-\frac{\left|W_i-H_i\sqrt{\frac{P}{L-m}}x_{p'_{\Omega_{j'}^{-1}(i)}}\right|^2}{N_0}}, & i\in\overline{\Omega}_j\cap\Omega_{j'}\\ 2e^{-\frac{|W_i|^2}{N_0}}, & i\in\overline{\Omega}_j\cap\overline{\Omega}_{j'}\end{cases} \tag{9}$$

TABLE II
CHANNEL PARAMETERS

Scenario	Velocity (km/h)	Doppler Shift (Hz)
Scenario 1	104	1000-1200
Scenario 2	32-48	300
Scenario 3	104	900-1150
Scenario 4	104	600-700
Scenario 5	32-48	400-500
Scenario 6	32-48	300-500

proposed in [22] and [23], which typically regarded as a standard V2X channel model dedicated for IEEE 802.11p. The measurement campaign was carried out in the metropolitan Atlanta, Georgia area including six scenarios, which are

- Scenario 1: V2V Expressway Oncoming;
- Scenario 2: V2V Urban Canyon Oncoming;
- Scenario 3: V2V Expressway Same Direction with Wall;
- Scenario 4: Roadside-to-vehicle (R2V) Expressway;
- Scenario 5: R2V Urban Canyon Oncoming; and
- Scenario 6: R2V Suburban Street.

The channel parameters for these six scenarios are listed in Table II. For brevity, we only present the results under Scenario 1, Scenario 3, and Scenario 5, which cover both V2V and R2V channels and a wide range of Doppler shifts.

2) BER Comparisons: In the simulations, the channel estimation is performed by the preamble, which is located prior to each OFDM data symbol and comprises an entire OFDM symbol known by both the transmitter and the receiver. Then, the channel estimates are used for the equalization and demodulation of the OFDM data symbol. We measure the BER achieved by the system adopting the LLR detector versus the SNR, which is defined as $P/\left[\left(L-m\right)N_0\right]$.

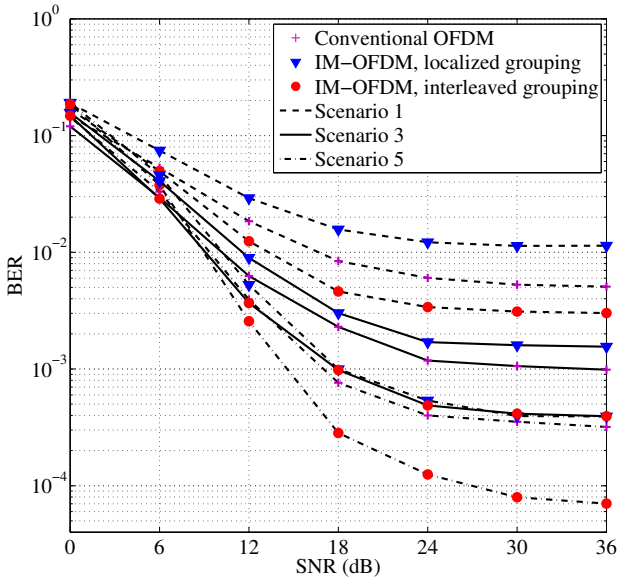

Fig. 5. BER performance for Scenario 1, Scenario 3, and Scenario 5 with $L=2$, $m=1$, and BPSK modulation.

Fig. 5 compares the uncoded BER of IM-OFDM with localized grouping and interleaved grouping for $L=2$, $m=1$, and BPSK modulation. The BER curves of conventional OFDM are also depicted for reference. Note that IM-OFDM with localized grouping for $L=2$ and $m=1$ is exactly the previous ESIM-OFDM scheme [16]. Also, for a fair comparison, we set parameters such that both IM-OFDM and conventional OFDM achieve the same transmitted information rate of 1 bps/Hz. As one can see from Fig. 5, unlike

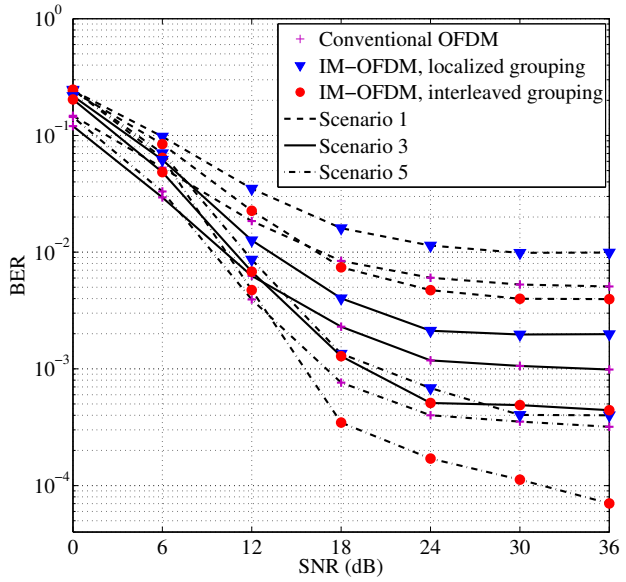

Fig. 6. BER performance for Scenario 1, Scenario 3, and Scenario 5 with $L = 4$, $m = 2$, and BPSK modulation.

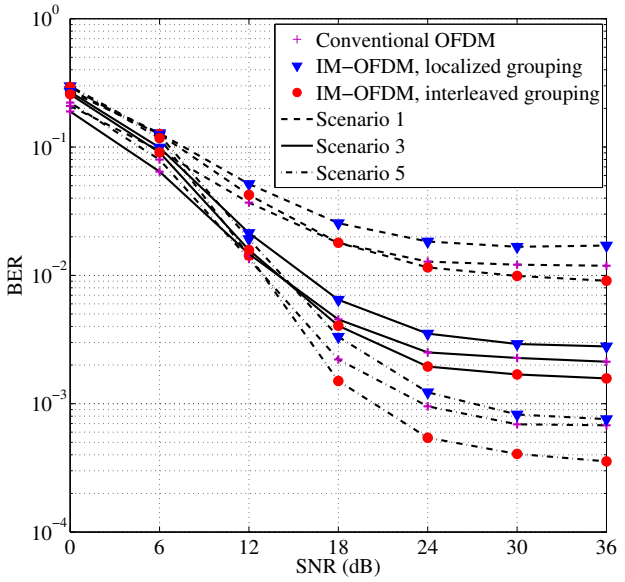

Fig. 7. BER performance for Scenario 1, Scenario 3, and Scenario 5 with $L = 4$, $m = 1$, and QPSK modulation.

conventional OFDM where the performance is irrelevant to the grouping type, the performance of IM-OFDM highly depends on the grouping method. With existing localized grouping, the IM-OFDM performance is even worse than the conventional OFDM. With our proposed interleaved grouping, the IM-OFDM outperforms conventional OFDM.

Also, notice that the performance difference between the two grouping methods starts to emerge even at fairly low SNR values. As the SNR increases, the performance gap between the two grouping methods becomes increasingly obvious. At very high SNR, the Doppler-induced ICI becomes the limiting factor, and thus all curves exhibit error floors. As detailed in Table II, Scenario 1 has the highest Doppler shift. Correspondingly, the BER error floors are the highest for all three schemes. However, it is worth mentioning that, our proposed IM-OFDM with interleaved grouping results in the most significant performance boost when the Doppler is relatively small. This is because interleaved grouping helps mitigate the detrimental Doppler effects by gathering subcarriers that are much further away than in the localized grouping. Clearly, this will be the most effective when the Doppler is moderate and does not propagate to further-apart subcarriers.

In IM-OFDM, the change of symbol modulation size can be offset by the subcarrier activation parameters to maintain the same transmitted information rate. Hence, alternative to the parameter set used to generate Fig. 5, one could use $L = 4$, $m = 2$, and BPSK modulation without affecting the transmitted information rate. The corresponding results are shown in Fig. 6. Comparing Figs. 5 and 6, we observe that the performance of conventional OFDM and IM-OFDM with localized grouping remains the same, whereas our IM-OFDM experiences a slight performance degradation with the new parameter set. This is yet another evidence that our performance advantage comes precisely from the inter-subcarrier spacing within the same subgroup, whereas the inter-subcarrier spacing in the $\{L = 2,\ m = 1\}$ case is slightly larger than the $\{L = 4,\ m = 2\}$ case.

Fig. 7 shows the comparison results for a spectral efficiency of 2 bps/Hz, where $L = 4$, $m = 1$, and QPSK modulation are assumed. From Fig. 7, we observe similar phenomenon to Figs. 5 and 6 except for a worse BER performance due to the adoption of a higher modulation order.

3) MAR Comparisons: Though the analysis in Section IV.A shows the advantage of interleaved grouping over localized grouping in terms of the MAR. However, that analysis assumes Rayleigh fading. In addition, the presence of Doppler in V2X channels further complicates the case and renders an analytical comparison impossible. Here we resort to a semi-simulated approach for an MAR comparison in V2X channels.

First notice that the MAR consists of two parts as we stated in Section IV.A, namely the symbol modulation and the subcarrier activation. We first consider the case with subcarrier activation only. Then for each channel realization, one can get the pairwise symbol-error rate (SER) averaged over additive noise realizations for IM-OFDM with different grouping methods respectively. Note that here the symbol cardinality (e.g., modulation size) equals to $\mathbb{C}(L, m)$. Now consider the case with symbol modulation on top of the subcarrier activation. But in decoding, we assume that the indices of activated subcarriers are known. Then we obtain the pairwise SER for the symbol modulations only, again for interleaved and co-located subcarrier grouping respectively. Then use these pairwise SER values in a discrete memoryless

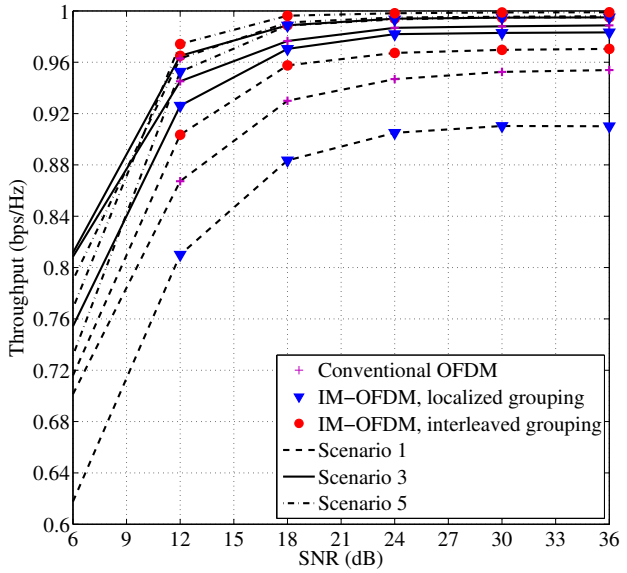

Fig. 8. Throughput performance for Scenario 1, Scenario 3, and Scenario 5 with $L = 2$, $m = 1$, and BPSK modulation.

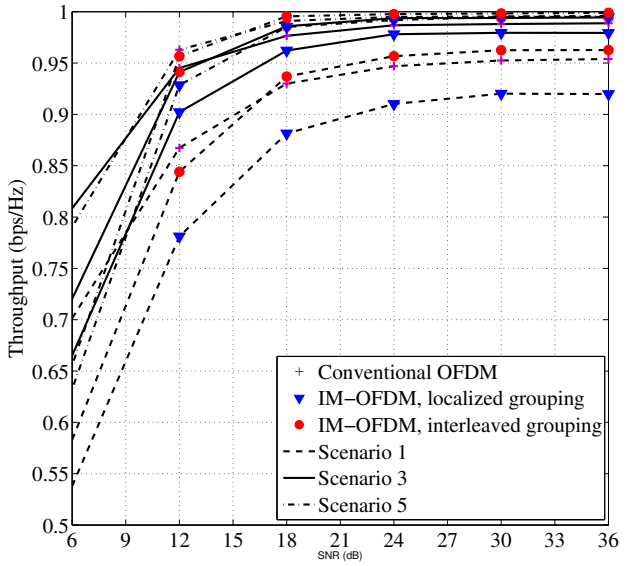

Fig. 9. Throughput performance for Scenario 1, Scenario 3, and Scenario 5 with $L = 4$, $m = 2$, and BPSK modulation.

channel (DMC) model [31], one can obtain the instantaneous (in the sense of channel realization) MI for the subcarrier activation part and the symbol modulation part. Combining these MI values and averaging over sufficient V2X channel realizations, we obtain the comparison results in Figs. 8-10 for all three different system parameter sets, respectively. It can be readily observed that, at medium-to-high SNR, our proposed IM-OFDM with interleaved grouping provides the highest throughput, validating our analysis in Section IV.A.

V. Conclusions

In this paper, an interleaved grouping method has been proposed for IM-OFDM to make it more suitable for V2X communications. We have shown that our proposed interleaved grouping method outperforms the existing localized grouping method in V2X channels with frequency-selective fading and Doppler. The benefits of our IM-OFDM with interleaved grouping in terms of BER and MAR performance have been revealed via analytical and simulated comparisons with respect to conventional OFDM as well as IM-OFDM with localized grouping.

Acknowledgement

This work was jointly supported by the National Natural Science Foundation of China (Grant No. 61101079, 61172105, and 61322107), the National 973 project (Grant No. 2013CB336700), the Science Foundation for the Youth Scholar of Ministry of Education of China (Grant No. 20110001120129), the National 863 Project (Granted No. 2014AA01A706), the Ministry of Transport of China (Grant No. 2012-364-X03-104), the Important National Science & Technology Specific Project of China (Grant No. 2013ZX03003006), the open research fund of National Mobil Communications Research Laboratory (Grant No. 2012D06), Southeast University, and the independent project of State Key Laboratory of Management and Control for Complex Systems (Grant No. Y3S9021F3D).

References

[1] F. Wang, D. Zeng, and L. Yang, "Smart cars on smart roads: An IEEE intelligent transportation systems society update," *IEEE Pervasive Computing*, vol. 5, no. 4, pp. 68–69, October-December, 2006.

[2] F. Qu, F. Wang, and L. Yang, "Intelligent transportation spaces: vehicles, traffic, communications, and beyond," *IEEE Commun. Mag.*, vol. 48, no. 11, pp. 136–142, November 2010.

[3] X. Cheng, X. Hu, L. Yang, I. Husain, K. Inoue, P. Krein, R. Lefevre, Y. Li, H. Nishi, J. Taiber, F. Wang, Y. Cha, W. Gao, and Z. Li, "Electrified vehicles and the smart grid: the ITS perspective," *IEEE Trans. on Intell. Transp. Syst.*, vol. 15, no. 4, pp. 1388-1404, Aug. 2014.

[4] M. Wen, X. Cheng, J. Wu, L. Yang, and B. Jiao, "Optimal correlative coding for discrete-time OFDM systems," *IEEE Trans. on Veh. Tech.*, vol. 63, no. 2, pp. 987-993, Feb. 2014.

[5] X. Shen, X. Cheng, L. Yang, R. Zhang, and B. Jiao, "Data dissemination in VANETs: a scheduling approach," *IEEE Trans. on Intell. Transp. Syst.*, 2014 (to appear).

[6] R. Zhang, X. Cheng, L. Yang, X. Shen, and B. Jiao, "A novel centralized TDMA-based scheduling protocol for vehicular networks," *IEEE Trans. on Intell. Transp. Syst.*, 2014 (to appear).

[7] *802.11p-2010 IEEE Standard for Information Technology?Telecommunications and Information Exchange Between Systems?Local and Metropolitan Area Networks?Specific Requirements Part 11*, Wireless LAN Medium Access Control (MAC) and Physical Layer (PHY) Spec, 2010.

[8] R. Mesleh, H. Haas, S. Sinanović, C. W. Ahn, and S. Yun, "Spatial modulation," *IEEE Trans. on Veh. Tech.*, vol. 57, no. 4, pp. 2228–2241, July 2008.

[9] M. Di Renzo, H. Haas, and P. M. Grant, "Spatial modulation for multiple-antenna wireless systems: a survey," *IEEE Commun. Mag.*, vol. 49, no. 12, pp. 182–191, Dec. 2011.

[10] M. Wen, X. Cheng, H. V. Poor, and B. Jiao, "Use of SSK modulation in two-way amplify-and-forward relaying," *IEEE Trans. on Veh. Tech.*, vol. 63, no. 3, pp. 1498-1504, Mar. 2014.

[11] Y. Bian, X. Cheng, M. Wen, L. Yang, H. V. Poor, and B. Jiao, "Differential spatial modulation," *IEEE Trans. on Veh. Tech.*, 2014 (to appear).

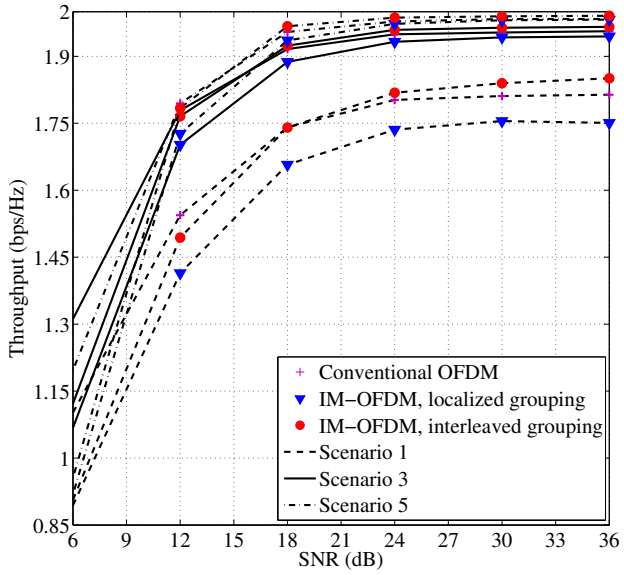

Fig. 10. Throughput performance for Scenario 1, Scenario 3, and Scenario 5 with $L = 4$, $m = 1$, and QPSK modulation.

[12] M. Di Renzo, H. Haas, A. Ghrayeb, S. Sugiura, and L. Hanzo, "Spatial modulation for generalized MIMO: Challenges, opportunities and implementation," *Proc. IEEE*, vol. 102, no. 1, pp. 56-103, Jan. 2014.

[13] X. Cheng, B. Yu, L. Yang, J. Zhang, G. Liu, Y. Wu, and L. Wan, "Communicating in the real world: 3D MIMO," *IEEE Wirel. Commun. Mag.*, vol. 21, no. 4, pp. 136-144, Aug. 2014.

[14] X. Cheng, C.-X. Wang, H. Wang, X. Gao, X.-H. You, D. Yuan, B. Ai, Q. Huo, L. Song, and B. Jiao, "Cooperative MIMO channel modeling and multi-link spatial correlation properties," *IEEE J. Sel. Areas in Commun.*, vol. 30, no. 2, pp. 388-396, Feb. 2012.

[15] R. A.Alhiga and H. Haas, "Subcarrier-index modulation OFDM," in *Proc. IEEE 20th International Symposium on Personal, Indoor and Mobile Radio Communications*, Tokyo, Japan, 2009, pp. 177-181.

[16] D. Tsonev, S. Sinanovic, and H. Haas, "Enhanced subcarrier index modulation (SIM) OFDM," in *Proc. IEEE GLOBECOM Workshops*, Houston, USA, 2011, pp. 728-732.

[17] E. Basar, U. Aygolu, E. Panayirci, and H. V. Poor, "Orthogonal frequency division multiplexing with index modulation," in *Proc. IEEE GLOBECOM*, Anahem, USA, 2012, pp. 4741–4746.

[18] E. Basar, U. Aygolu, and E. Panaylrcl, "Orthogonal frequency division multiplexing with index modulation in the presence of high mobility," in *Proc. IEEE First International Black Sea Conference on Communications and Networking (BlackSeaCom)*, 2013, pp. 147–151.

[19] E. Basar, U. Aygolu, E. Panayirci, and H. V. Poor, "Orthogonal frequency division multiplexing with index modulation," *IEEE Trans. on Signal Process.*, vol. 61, no. 22, pp. 5536-5549, Nov. 2013.

[20] M. Wen, X. Cheng, M. Wang, B. Ai, and B. Jiao, "Error probability analysis of interleaved SC-FDMA systems over Nakagami-m frequency selective fading channels," *IEEE Trans. on Veh. Tech.*, vol. 62, no. 2, pp. 748–761, Feb. 2013.

[21] M. Wen, X. Cheng, M. Ma, B. Jiao, and H. V. Poor, "On the maximum achievable rate of OFDM with index modulation," *IEEE Trans. on Signal Process.*, submitted for publication.

[22] G. Acosta-Marum and M. A. Ingram, "Six time- and frequency-selective empirical channel models for vehicular wireless LANs," *IEEE Veh. Tech. Mag.*, vol. 2, no. 4, pp. 4?-11, Dec. 2007.

[23] X. Cheng, C.-X. Wang, B. Ai, and H. Aggoune, "Envelope level crossing rate and average fade duration of non-isotropic vehicle-to-vehicle Ricean fading channels," *IEEE Trans. on Intell. Transp. Syst.*, vol. 15, no. 1, pp. 62-72, Feb. 2014.

[24] I. Sen and D. W. Matolak, "Vehicle-vehicle channel models for the 5-GHz band," *IEEE Trans. on Intell. Transp. Syst.*, vol. 9, no. 2, pp. 235?-245, Jun. 2008.

[25] X. Cheng, Q. Yao, M. Wen, C.-X. Wang, L. Song, and B. Jiao, "Wideband channel modeling and ICI cancellation for vehicle-to-vehicle communication systems," *IEEE J. Sel. Areas in Commun.*, vol. 31, no. 9, pp. 434-448, Sept. 2013.

[26] X. Cheng, Q. Yao, C.-X. Wang, B. Ai, G. L. Stuber, D. Yuan, and B. Jiao, "An improved parameter computation method for a MIMO V2V Rayleigh fading channel simulator under non-isotropic scattering environments," *IEEE Commun. Lett.*, vol. 17, no. 2, pp. ?65 -268, Feb. 2013.

[27] J. Karedal, F. Tufvesson, N. Czink, A. Paier, C. Dumard, T. Zemen, C. F. Mecklenbrauker, and A. F. Molisch, "A geometry-based stochastic MIMO model for vehicle-to-vehicle communications," *IEEE Trans. on Wirel. Commun.*, vol. 8, no. 7, pp. 3646-3657, Jul. 2009.

[28] X. Cheng, C. -X. Wang, D. I. Laurenson, S. Salous, and A. V. Vasilakos, "An adaptive geometry-based stochastic model for non-isotropic MIMO mobile-to-mobile channels," *IEEE Trans. on Wirel. Commun.*, vol. 8, no. 9, pp. 4824-4835, Sep. 2009.

[29] X. Cheng, C.-X. Wang, D. Laurenson, S. Salous, and A. Vasilakos, "New deterministic and stochastic simulation models for non-isotropic scattering mobile-to-mobile Rayleigh fading channels," *Wireless Communications and Mobile Computing*, John Wiley & Sons, vol. 11, no. 7, pp. 829-842, Jul. 2011.

[30] C.-X. Wang, X. Cheng, and D. Laurenson, "Vehicle-to-vehicle channel modeling and measurements: recent advances and future challenges," *IEEE Commun. Mag.*, vol. 47, no. 11, pp. 96-103, Nov. 2009.

[31] T. M. Cover and J. A. Thomas, *Elements of Information Theory*. New York, NY: John Wiley & Sons, 1991.